Catena 124 (2015) 9–17

Contents lists available at ScienceDirect

Catena

journal homepage: www.elsevier.com/locate/catena

Land use impacts on soil detachment capacity by overland flow in the Loess Plateau, China

Zhen-Wei Li [a,b], Guang-Hui Zhang [a,c,*], Ren Geng [c], Hao Wang [c], X.C. Zhang [d]

[a] State Key Laboratory of Soil Erosion and Dryland Farming on the Loess Plateau, Institute of Soil and Water Conservation, Chinese Academy of Sciences and Ministry of Water Resources, Yangling, Shaanxi 712100, China
[b] University of Chinese Academy of Sciences, Beijing 100049, China
[c] School of Geography, Beijing Normal University, Beijing 100875, China
[d] USDA-ARS Grazinglands Research Laboratory, EL Reno, OK, USA

ARTICLE INFO

Article history:
Received 5 July 2014
Received in revised form 14 August 2014
Accepted 27 August 2014
Available online xxxx

Keywords:
Soil erosion
Detachment capacity
Soil type
Land use
The Loess Plateau

ABSTRACT

Land use and its adjustment may greatly affect soil detachment process by overland flow via altering soil properties, root systems, and tillage operations, but few studies were performed to quantify their effects on soil detachment in the Loess Plateau. This study was conducted to investigate the potential effects of land use on soil detachment capacity by overland flow (D_c, kg m^{-2} s^{-1}) using natural undisturbed soil samples taken from four different land uses on the red loess soil and six different land uses on the yellow loess soil, and to quantify the relationships between soil detachment capacity and hydraulic parameters, soil properties, and root systems in the Loess Plateau. The collected samples were tested in a 4.0 m long, 0.35 m wide hydraulic flume under six different shear stresses (5.51–16.59 Pa). The result showed that both soil type and land use had significant effects on D_c. For two tested soils, the mean D_c of the yellow loess soil was 1.49 times greater than that of the red loess soil. For the red loess soil, D_c of cropland was the maximum, which was 5.57, 5.85, and 34.08 times greater than those of shrub land, orchard, and grassland, respectively. For the yellow loess soil, cropland was much more erodible than other five land uses. On average, the ratios of the cropland D_c to those of orchard, shrub land, woodland, grassland, and wasteland were 7.14, 12.29, 25.78, 28.45, and 46.43, respectively. The variability of D_c under different land uses was closely related to soil properties, root systems, and tillage operations. Soil detachment capacity was positively related to silt content, and inversely related to sand content, cohesion, water stable aggregate, aggregate median diameter, organic matter, and root density. The measured detachment capacity could be well estimated by measurable parameters of stream power, slope gradient, soil bulk density, median diameter, silt content, cohesion, and root density (Nash–Sutcliffe efficiency = 0.89).

1. Introduction

Soil detachment, defined as the soil particles being separated from the soil matrix at a particular location on the soil surface by erosive agents (Wang et al., 2014a; Zhang et al., 2003), is a key process affecting soil erosion since it determines the amount of sediment that is potentially transferred to surface water bodies. Soil detachment rate is expressed as the sediment amount detached per unit area per unit time (Zhang et al., 2009a). With increase in sediment concentration in flowing water, more energy is used for sediment transport, which causes a decrease in soil detachment rate (Lei et al., 2002; Zhang et al., 2009b). The maximum soil detachment rate occurs in the case of clear water and it is termed as soil detachment capacity (Nearing et al., 1991). Soil detachment capacity is a key parameter in many process-based erosion models such as the Water Erosion Prediction Project (WEPP) model (Nearing et al., 1989). Therefore, quantifying D_c under different conditions is pivotal to calibrate and validate the process-based erosion models.

Soil detachment capacity by overland flow is influenced by various factors such as flow hydraulics, soil properties, root systems, tillage operations, and land use (Knapen et al., 2007a; Scherer et al., 2012). For a given soil, flow hydraulics (e.g. discharge, slope gradient, flow depth, and velocity) control the process of detachment (Govers, 1992; Zhang et al., 2003). Soil detachment capacity increases with flow discharge and slope gradient, and is more sensitive to discharge than slope gradient. Shear stress and stream power are commonly used to simulate erosion processes in process-based models (Nearing et al., 1991). However, some studies indicate that stream power is better than shear stress to predict soil detachment capacity (Cao et al., 2009; Zhang et al., 2003).

* Corresponding author at: State Key Laboratory of Soil Erosion and Dryland Farming on the Loess Plateau, Institute of Soil and Water Conservation, Chinese Academy of Sciences and Ministry of Water Resources, Yangling, Shaanxi 712100, China. Tel.: +86 13671086156; fax: +86 10 58806955.
E-mail address: ghzhang@bnu.edu.cn (G.-H. Zhang).

http://dx.doi.org/10.1016/j.catena.2014.08.019

Soil detachment capacity is strongly influenced by soil properties since it occurs on the interface of flowing water and soil (Zhang et al., 2009a). D_c decreases with increases in clay content, bulk density, cohesion, water stable aggregate, aggregate median diameter, organic matter content, and biological crust (Ghebreiyessus et al., 1994; Knapen et al., 2007a, 2007b; Wang et al., 2013; Zhang et al., 2008), but increases with silt content and soil moisture (Knapen et al., 2007a; Nachtergaele and Poesen, 2002). In a flume experiment using disturbed soil samples, Ciampalini and Torri (1998) found that soil detachment capacity could be predicted by clay content, bulk density, shear strength, and aggregate median diameter. For undisturbed soil samples, De Baets and Poesen (2010) showed that bulk density and soil moisture could be used to estimate D_c for both bare and rooted topsoils.

Plant root is another important factor affecting soil detachment capacity by overland flow via its physically binding effect and chemically bonding effect to enhance soil stability and resistance to flowing water erosion (Wang et al., 2014b). Root systems also play a crucial role to improve soil strength, thereby reducing the erodibility of topsoil (De Baets et al., 2011). Soil detachment capacity decreases exponentially with increasing root mass density (De Baets et al., 2006; Zhang et al., 2013). Root architecture also has a great influence on the role of roots to control soil erosion by flowing water. Fibrous root systems are more powerful to reduce soil detachment than tap root systems (De Baets et al., 2007).

Tillage operations (e.g. planting, plowing, hoeing, and harvesting) disturbed land surface to form a loose erodible layer and hence promotes soil detachment capacity (Zhang et al., 2009a). With time elapsing after tillage, the topsoil consolidates and is difficult to detach by flowing water due to the effect of consolidation, resulting a decrease in soil detachment capacity (Knapen et al., 2007a; Zhang et al., 2009a). In a field study, King et al. (1995) found that soil detachment rate was much lower in a no-till soil than that in a conventional-till soil. In eroding channels with high-discharge overland flow, Franti et al. (1999) demonstrated that soil detachment rates from tilled channels were an order of magnitude greater than those from no-till channels.

Many studies showed that land use has a profound influence on soil erosion (García-Ruiz, 2010; Podwojewski et al., 2008). Among the factors related to the intensity and frequency of flowing water erosion, land use is considered as the most important factor influencing soil detachment, even exceeding the influence of rainfall intensity and slope gradient in some circumstances (García-Ruiz, 2010). Soil detachment capacity by overland flow may vary widely under different land uses (Ciampalini and Torri, 1998; Knapen et al., 2007a), yet few studies have been conducted to quantify the differences. The study conducted by Zhang et al. (2008) found that soil detachment capacity was affected by land use considerably. The D_c of cropland was the maximum and was 2.05, 2.76, 3.32, and 13.32 times greater than those of grassland, shrub land, wasteland, and woodland, respectively.

As one of the severely eroded region, the Chinese Loess Plateau probably has the most severe erosion in the world, which directly restricts the ecological security and the social economical sustainability in this area (Fu et al., 2000). The principal reason for such serious erosion in the Loess Plateau is low vegetation cover as a result of inappropriate land use (Fu et al., 2000). Therefore, the Chinese government has paid great attention to control soil erosion in this region. The long-term, policy-driven "Grain for Green" project implemented in 1999 is mainly to plant trees, grass, or to convert croplands to grasslands under natural vegetation restoration to reduce soil erosion and improve soil quality in the Loess Plateau (Fu et al., 2000, 2006). This project must lead to great changes in land use, and thus results in potential changes in soil detachment process.

Land use adjustment certainly causes, at least at a small watershed scale, many changes in soil properties (Celik, 2005; Islam and Weil, 2000), root systems (Burylo et al., 2012; Pierret et al., 2007), and tillage operations (Knapen et al., 2007a; Zhang et al., 2009a). Those changes affect soil detachment diversely as mentioned above. However, the impact of land use on soil detachment capacity is not yet fully quantified, especially in a landscape where the complex combinations of soil type, land use, and plant species could certainly affect soil detachment capacity by overland flow. The objectives of this study were to investigate the potential effects of land use on soil detachment capacity by overland flow using undisturbed soil samples collected from the red loess and yellow loess soils subjected to detach under different hydraulic conditions, and to quantify the relationships between soil detachment capacity and hydraulic parameters, soil properties, and root systems in a Loess Plateau catchment.

2. Materials and methods

2.1. Study area

Experiments were carried out in the Zhifanggou watershed in Ansai County, Shaanxi Province, China (36°46′28″–36°46′42″N, 109°13′46″–109°16′03″E, altitude 1010–1431 m) (Fig. 1). The watershed is 8.27 km^2 in size and is characterized by a semiarid continental climate, with the mean annual temperature and precipitation of 8.8 °C and 505 mm. The geomorphology exhibits the characteristics of a main valley with a gully density of 4.20 to 8.06 km km^{-2} (Fu et al., 2006). The soil, developed from loess parent material, has a homogeneous silt loam texture, and is weakly resistant to erosion (Fu et al., 2006). The yellow loess soil and red loess soil are two main soil types in the watershed and their major properties are shown in Table 1. Due to long-term intensive human activities, most natural vegetation has been destroyed. Current principal land uses are cropland, orchard, shrub land, woodland, grassland, and wasteland. The major plant species of different land uses are listed in Table 1.

2.2. Sampling site

After a completely watershed survey, the sampling sites were stratified by soil types, land uses, and plant species. Altogether 23 sampling sites (including 6 land uses, 23 plant species) and 6 sampling sites (including 4 land uses, 6 plant species) were chosen for the yellow loess soil and red loess soil (Table 1, Fig. 1). Some weeds grew in shrub land and woodland, but few or none in cropland and orchard. Tillage operations such as planting, plowing, hoeing, and harvesting were operated in croplands, while no any tillage operations were utilized in shrub land, woodland, grassland, and wasteland. In orchard, weeds were hoed once in the jujube on yellow loess soil. A thin layer of soil biological crust was developed in the jujube orchard on red loess soil and on the YWaAA wasteland site (Table 1) when soil samples were taken, which probably had some effect on soil detachment capacity measurement.

2.3. Soil sampling

Undisturbed soil samples were collected from surface soil using steel rings with a diameter of 10 cm and a height of 5 cm from August to September 2013 for soil detachment capacity measurement. Detailed information of soil sampling procedures could be found in previous papers (Zhang et al., 2003, 2008, 2009a). The procedures were described briefly here. The sampling procedures were almost the same for all sites except for the treatment of weeds. In shrub land, woodland, grassland, and wasteland, the weeds were clipped carefully near the soil surface with a pair of scissors, and thus some roots existed in soil samples. In cropland and orchard, soil samples were collected from flat patches, and few roots were taken within soil samples. When sample was taking, the steel ring was slowly pressed down into the soil, and was excavated carefully after the top rim of the ring was flushed with the soil surface. Then the core bottom was trimmed to level with the ring rims, and both ends were covered with cotton cushions and lids to avoid disturbance during sample transport. To ensure the same soil moisture, the soil cores were saturated for 8 h in a container with a

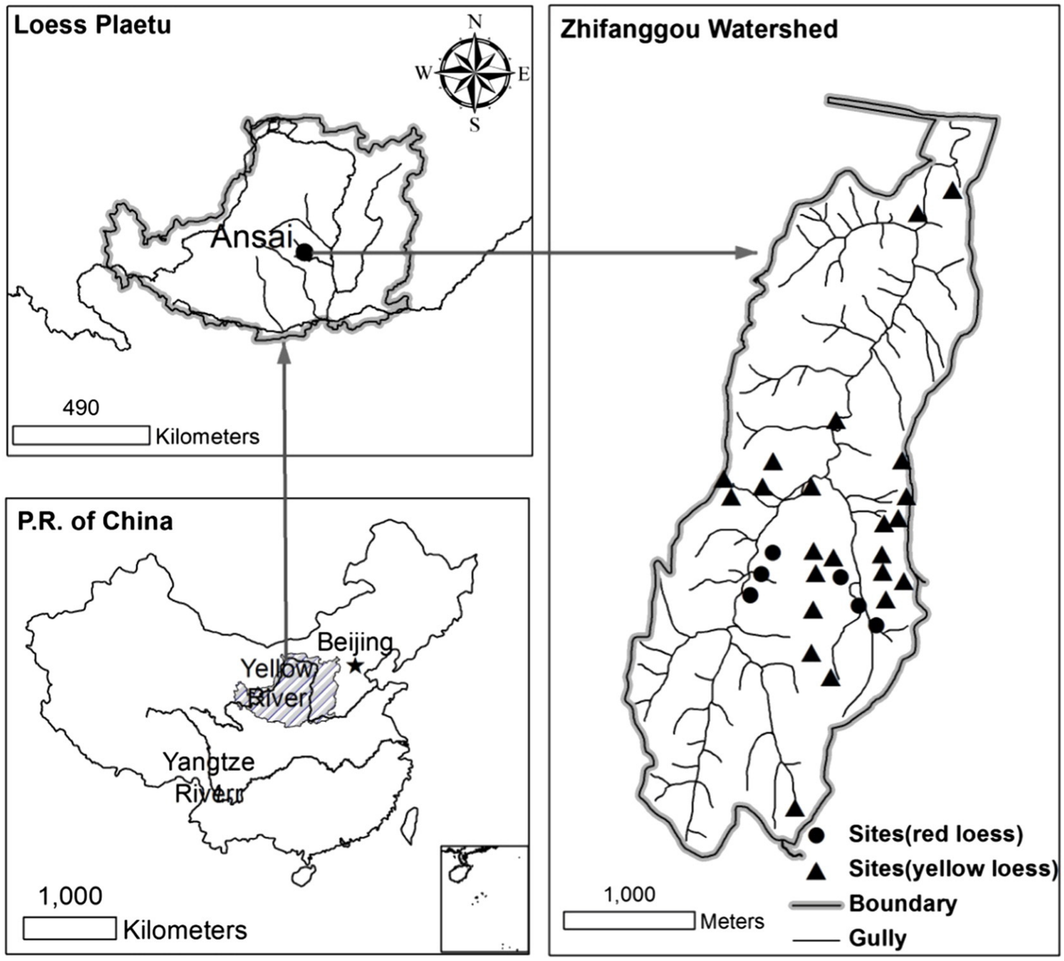

Fig. 1. Locations of the study watershed and the sampling sites.

water level of 1 cm below the top soil surface, and then drained for 12 h for soil detachment capacity measurement.

Additional soil samples were collected for each site to determine bulk density, particle size distribution, water stable aggregate, organic matter content, and root density. Soil bulk density was measured by the oven-drying method with three replicates. Soil particle size distribution was determined using a Mastersizer 2000 (Malvern Instruments, Malvern, England) with three replicates and then the median soil grain size was calculated. Water stable aggregate was measured by the wet-sieving method with three replicates. The aggregate median diameter was computed from the size distribution of aggregates (Wang et al., 2012). Soil organic matter was measured using the potassium dichromate colorimetric method for three replicates. After soil surface was saturated by a light sprayer, soil cohesion was measured ten times using a torvane (Durham Geo-enterprises, Inc., UK). Soil moisture was measured by the oven-dry method in six replicates taken around the sampling point and the mean value was used to compute the original dry mass of each soil sample. The mean values were used to represent soil properties for each sampling site (Table 1).

2.4. Hydraulic parameter measurement

The soil detachment capacity was measured in a 4.0 m long and 0.35 m wide hydraulic flume. The yellow loess soil (passing 2 mm sieve) was glued on the flume bed to simulate natural grain roughness. The slope of the flume could be adjusted manually. Flow discharge was controlled by five valves and measured five times with plastic buckets and a volumetric cylinder. After the flow became stable, the flow surface velocity was measured using a fluorescent dye technique for ten times, and the average was multiplied by a reduction factor of 0.8 to obtain the mean flow velocity (Luk and Merz, 1992). Flow depth was calculated using mean velocity as:

$$H = \frac{Q}{BV} \tag{1}$$

where H is the flow depth (m), Q is the flow discharge (m^3 s^{-1}), B is the width of flume (m), and V is the mean flow velocity (m s^{-1}). To measure soil detachment capacity under a wide range of flow hydraulics, six combinations of slope gradient (17.4%–42.3%) and unit width flow discharge (0.0029–0.0071 m^2 s^{-1}) were utilized in this study. Flow shear stress (5.51–16.59 Pa) and stream power (4.86–29.58 kg s^{-3}) were calculated as follows:

$$\tau = \rho g H S \tag{2}$$

where τ is the flow shear stress (Pa), ρ is the water mass density (kg m^{-3}), g is the gravity constant (m s^{-2}), and S is the slope gradient (m m^{-1}).

$$\omega = \tau V = \rho g H S V \tag{3}$$

where ω is the stream power (kg s^{-3}). The hydraulic parameters used in this study are presented in Table 2.

Table 1
Soil properties and root mass density of each sampling site.

Site code	Land use	Dominant plant species	Soil texture			Median soil grain size (μm)	Bulk density (kg m^{-3})	Soil cohesion (kPa)	Water stable aggregate (0–1)	Aggregate median diameter (mm)	Soil organic matter (g kg^{-1})	Root mass density (kg m^{-3})
			Clay (%)	Silt (%)	Sand (%)							
Red loess soil												
RCC	Cropland	Corn	18.19	71.16	10.66	17.77	1441 ± 5	7.66 ± 0.22	0.29 ± 0.01	0.79	5.52 ± 0.01	0.16 ± 0.04
ROA	Orchard	Apple	17.53	69.11	13.36	24.28	1307 ± 26	9.92 ± 0.43	0.44 ± 0.07	0.69	9.66 ± 0.01	0.37 ± 0.09
ROJ		Jujube	26.84	67.55	5.61	10.40	1388 ± 41	10.21 ± 0.37	0.65 ± 0.04	3.26	12.36 ± 0.01	0.34 ± 0.16
RSS	Shrub land	Sea-buckthorn	18.01	65.73	16.26	19.24	1309 ± 58	9.98 ± 0.18	0.57 ± 0.02	2.35	10.74 ± 0.03	0.97 ± 0.21
RGA	Grassland	*Artemisia sacrorum*	19.17	65.70	15.13	16.24	1547 ± 21	10.53 ± 0.18	0.44 ± 0.03	0.87	13.78 ± 0.05	4.52 ± 0.61
RGB		*Bothriochloa ischaemum*	12.21	55.51	32.28	31.04	1477 ± 16	11.29 ± 0.22	0.74 ± 0.07	3.76	25.01 ± 0.05	7.41 ± 0.52
Yellow loess soil												
YCC	Cropland	Corn	11.18	68.23	20.58	28.65	1320 ± 6	7.45 ± 0.23	0.27 ± 0.02	1.26	4.98 ± 0.04	0.20 ± 0.04
YCM		Millet	9.61	66.76	23.63	37.22	1165 ± 7	8.19 ± 0.19	0.26 ± 0.03	1.19	6.28 ± 0.02	0.23 ± 0.03
YCP		Potato	11.08	70.77	18.15	30.96	1270 ± 19	8.04 ± 0.36	0.17 ± 0.01	1.66	7.78 ± 0.14	0.28 ± 0.06
YCS		Soybean	12.16	68.29	19.55	30.00	1191 ± 23	8.70 ± 0.19	0.37 ± 0.01	0.60	6.05 ± 0.05	0.15 ± 0.02
YOA	Orchard	Apple	13.10	68.02	18.88	26.28	1215 ± 27	9.84 ± 0.30	0.26 ± 0.03	0.81	10.08 ± 0.12	0.28 ± 0.06
YOH		Hawthorn	9.77	60.21	30.02	36.42	1346 ± 18	12.52 ± 0.32	0.43 ± 0.01	2.54	9.89 ± 0.06	0.42 ± 0.13
YOJ		Jujube	16.71	67.23	16.06	20.77	1391 ± 60	12.88 ± 0.27	0.56 ± 0.05	1.82	11.24 ± 0.05	0.38 ± 0.06
YOW		Walnut	8.96	63.33	27.71	35.61	1210 ± 64	10.84 ± 0.24	0.47 ± 0.01	2.42	16.45 ± 0.14	0.99 ± 0.11
YSK	Shrub land	Korshinsk peashrub	7.99	61.17	30.85	38.27	1049 ± 13	10.96 ± 0.23	0.42 ± 0.01	2.06	16.93 ± 0.17	0.93 ± 0.13
YSSB		Sea-buckthorn	10.23	61.09	28.69	35.32	1217 ± 32	12.56 ± 0.33	0.40 ± 0.01	2.09	10.40 ± 0.07	1.58 ± 0.23
YSSD		*Sophora davidii*	9.14	63.92	26.94	33.28	1335 ± 29	12.52 ± 0.35	0.61 ± 0.01	3.18	17.70 ± 0.03	1.27 ± 0.13
YWB	Woodland	Black locust	12.83	67.34	19.83	27.51	1310 ± 2	12.82 ± 0.37	0.51 ± 0.03	2.73	8.14 ± 0.10	1.46 ± 0.24
YWC		Chinese pine	8.33	61.07	30.61	38.32	1155 ± 40	13.01 ± 0.24	0.45 ± 0.02	2.32	10.07 ± 0.04	1.21 ± 0.18
YWS		Simon poplar	15.65	63.13	21.22	22.44	1463 ± 25	13.25 ± 0.27	0.63 ± 0.02	3.33	20.55 ± 0.16	2.18 ± 0.24
YGAA	Grassland	*Astragalus adsurgens*	12.65	62.16	25.19	28.60	1196 ± 28	12.94 ± 0.27	0.68 ± 0.01	3.84	17.79 ± 0.01	4.93 ± 0.54
YGAC		*Artemisia capillaris*	10.78	67.10	22.11	29.97	1307 ± 30	12.15 ± 0.42	0.43 ± 0.02	2.37	9.62 ± 0.07	1.70 ± 0.22
YGAS		*Artemisia sacrorum*	7.70	60.0	32.30	38.44	1165 ± 55	10.98 ± 0.27	0.33 ± 0.01	1.33	28.15 ± 0.23	0.72 ± 0.15
YGBI		*Bothriochloa ischaemum*	9.74	58.43	31.83	37.73	1432 ± 23	11.92 ± 0.42	0.55 ± 0.02	2.80	12.87 ± 0.15	5.51 ± 0.81
YGCL		*Carex lanceolata*	9.63	61.09	29.27	36.41	1252 ± 9	12.60 ± 0.39	0.38 ± 0.02	1.75	8.22 ± 0.02	5.90 ± 0.79
YGSB		*Stipa bungeana*	14.46	59.56	25.97	30.23	1192 ± 6	12.68 ± 0.40	0.40 ± 0.01	1.68	10.48 ± 0.09	2.42 ± 0.25
YGSV		*Setaria viridis*	10.18	59.95	29.87	35.01	1247 ± 19	12.39 ± 0.29	0.58 ± 0.06	2.74	23.60 ± 0.12	1.87 ± 0.15
YWaAA	Wasteland	*Astragalus adsurgens* + *Artemisia sacrorum*	10.31	59.00	30.69	35.15	1245 ± 2	12.52 ± 0.32	0.46 ± 0.03	2.41	14.30 ± 0.16	0.48 ± 0.07
YWaBS		*Bothriochloa ischaemum* + *Setaria viridis*	9.28	61.71	29.01	34.13	1404 ± 31	12.37 ± 0.39	0.58 ± 0.03	3.29	24.15 ± 0.05	3.30 ± 0.32

2.5. Soil detachment capacity measurement

Prior to each test, the flow discharge and flume slope gradient were adjusted to designed values. The pre-saturated soil sample was inserted in a circle hole on the flume bed, located at a distance of 0.5 m from the lower end of flume, with the sample surface flush with the flume bed. Then the soil detachment capacity measurement started, and the test lasted no more than 300 s for each sample. When the scouring depth reached 2 cm, the test was stopped to prevent the boundary effects from sampling ring (Knapen et al., 2007b; Nearing et al., 1991). After each test, the soil sample was oven dried at 105 °C for 12 h and weighted to determine the final oven dry mass. Soil detachment capacity (D_c, kg m^{-2} s^{-1}) was calculated as:

$$D_c = \frac{M_o - M_f}{At} \tag{4}$$

where M_o is the original dry mass of soil sample (kg, weight of wet soil sample minus the water weight), M_f is the final oven-dry mass of soil sample (kg), A is the cross-section area of soil sample (m^2), and t is the test period (s). For each shear stress, soil detachment capacity was measured for four replicates and the mean was considered as the soil detachment capacity for that shear stress and sampling site. Altogether, 696 samples were tested. After each test, roots within each soil sample were collected by washing over a sieve (1 mm) and weighted after oven-drying for 12 h at 65 °C.

Table 2
Hydraulic parameters used in this study.

Flow discharge (m^2 s^{-1})	Slope gradient (%)	Mean flow velocity (m s^{-1})	Flow depth (mm)	Shear stress (Pa)	Stream power (kg s^{-3})
0.0029	17.4	0.88	3.2	5.51	4.86
0.0057	17.4	1.10	5.2	8.81	9.72
0.0057	25.9	1.41	4.1	10.26	14.49
0.0043	42.3	1.42	3.0	12.51	17.75
0.0057	42.3	1.59	3.6	14.88	23.67
0.0071	42.3	1.78	4.0	16.59	29.58

2.6. Statistical analysis

Significant differences of the mean soil detachment capacity between soil types, land uses, and plant species were detected using a one-way analysis of variance (ANOVA) followed by LSD ($p < 0.05$) and two-way ANOVA analysis. Relationships between soil detachment capacity and flow hydraulics, soil properties or root mass density were analyzed by a simple regression method. A non-linear regression method was used to estimate the relationships between soil detachment capacity and hydraulic parameters, soil properties, and root mass density. The regression results were evaluated by the coefficient of determination and Nash–Sutcliffe model efficiency. All statistical analyses were conducted in SPSS 17.0.

3. Results and discussion

3.1. Soil type impacts on soil detachment capacity

Two-way ANOVA analysis indicated that soil detachment capacity was influenced by soil type, land use, and their interaction significantly

($p < 0.01$). For comparison, the detachment capacities under six shear stresses were averaged for each land use. In most cases (66.7%), soil type influenced soil detachment capacity significantly (Fig. 2). Soil detachment capacity of the yellow loess soil was 1.49 times greater than that of the red loess soil. The ratios of soil detachment capacity in corn, apple, jujube, *Artemisia sacrorum*, and *Bothriochloa ischaemum* fields of the yellow loess soil to those of the red loess soil were 1.34, 1.32, 8.65, 2.46, and 6.71, respectively. The difference in soil detachment capacity between two soils was probably caused by the differences in the clay content and bulk density, which were reversely related to soil detachment. The average clay content and bulk density were 18.66% and 1412 kg m^{-3} for the red loess soil; whereas they were 11.44% and 1290 kg m^{-3} for the yellow loess soil. Thus the low measured D_c for the yellow loess soil was expected. No significant differences between two soil types in apple fields can be explained as follows. First, the large variations between shear stress groups were treated as within-treatment variances. If the tests were conducted for each shear stress level, the results were significant. Second, the weeds were hoed in apple fields for high productivity, which certainly disturbed land surface and thus reduced the influence of soil type on detachment. It was well known that soil detachment rate declined with root density via its physically binding and chemical bonding effects (De Baets et al., 2006; Zhang et al., 2013). In this study, the root mass density in sea-buckthorn land of the yellow loess soil was 1.63 times greater than that of the red loess soil, which led to the low measured D_c in the yellow loess soil.

3.2. Land use impacts on soil detachment capacity

3.2.1. Red loess soil

As shown in Fig. 3, it was obvious that land use affected soil detachment capacity of the red loess soil significantly except for the difference between *A. sacrorum* and jujube lands. On average, soil detachment capacity of corn was the maximum (0.81 kg m^{-2} s^{-1}), and followed by shrub land (0.14 kg m^{-2} s^{-1}), orchard (0.14 kg m^{-2} s^{-1}), and grassland (0.02 kg m^{-2} s^{-1}). The mean detachment capacities of shrub land and orchard were almost the same since the measured D_c of jujube land (as an orchard) was very low that was caused by soil biological crust development (Knapen et al., 2007b; Wang et al., 2013).

3.2.2. Yellow loess soil

Similarly, land use influenced soil detachment capacity of the yellow loess soil considerably (Fig. 4). The mean soil detachment capacity of cropland (1.31 kg m^{-2} s^{-1}) was the maximum among the six land uses and was 7.14, 12.29, 25.78, 28.45, and 46.43 times greater than

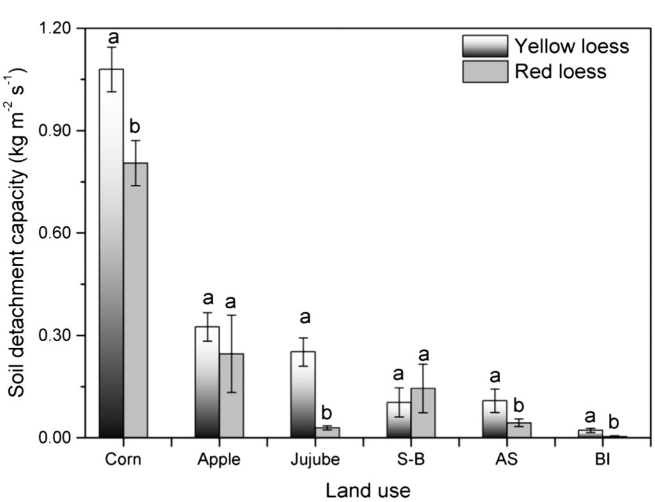

Fig. 2. Comparison of soil detachment capacities between yellow loess and red loess soils (S-B: sea-buckthorn, AS: *Artemisia sacrorum*, and BI: *Bothriochloa ischaemum*.). Error bars represent the standard deviation.

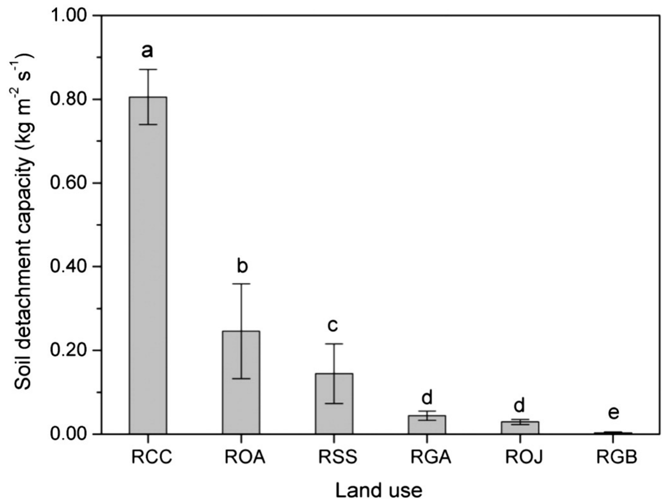

Fig. 3. Comparison of soil detachment capacities between different land uses on red loess soil. Error bars represent the standard deviation.

those of orchard, shrub land, woodland, grassland, and wasteland, respectively. This result agreed with the conclusion of previous studies that land use had a significant impact on soil detachment capacity and the cropland was the most erodible land use in the Loess Plateau (Zhang et al., 2008, 2009a).

For four croplands, soil detachment capacity of potato was the maximum, followed by soybean, corn, and millet (Fig. 4A). The measured detachment capacity of croplands (0.03–4.43 kg m^{-2} s^{-1}) was an order magnitude greater than the data (0.002–0.311 kg m^{-2} s^{-1}) reported by Wang et al. (2012), although almost the same hydraulic conditions were utilized. This difference was probably caused by the differences in soil properties and the size of the soil sample. Loess soil used in this study was much more erodible than purple soil utilized in the study of Wang et al. (2012). Meanwhile, the length of soil samples was 39 cm in their study and low measured D_c was expected due to the sediment feedback effect on soil detachment capacity (Zhang et al., 2009b).

For four orchard lands, the weeds were hoed in apple and jujube lands, but no any operation was applied in hawthorn and walnut lands. Thus the measured detachment capacities of the former were significantly greater than the latter (Fig. 4A). For shrub lands, soil detachment capacity of korshinsk peashrub was the maximum that was caused by low root density and differed significantly from sea-buckthorn and *Sophora davidii* lands (Fig. 4A). For three wood lands, soil detachment capacities of black locust and simon poplar were 2.53 and 2.13 times greater than that of Chinese pine land (Fig. 4B). This difference was probably related to the restoration ages, which were 7, 18, and 38 years for black locust, simon poplar, and Chinese pine, respectively. Soil detachment capacity declined sharply when cropland was just abandoned and the relative stable stage was reached after 28 years (Wang et al., 2013). The measured soil detachment capacities of shrub land and woodland were similar to the results of Zhang et al. (2008).

For seven grasslands, *Stipa bungeana* had the maximum soil detachment capacity (0.12 kg m^{-2} s^{-1}) and was 1.05 to 9.28 times greater than the other six grasslands (Fig. 4B). No significant difference was found between *S. bungeana* and *A. sacrorum*. *Artemisia capillaris* differed with other six grasslands significantly. No significant difference was detected between *B. ischaemum* and *Setaria viridis*, *Astragalus adsurgens* and *Carex lanceolata* (Fig. 4B). The measured soil detachment capacities of seven grasslands varied from 0.001 to 0.309 kg m^{-2} s^{-1}, which were considerably greater than those reported by Mamo and Bubenzer (2001). Those differences were probably attributed to the differences in hydraulic conditions and soil properties. For two wastelands, the soil detachment capacity measured in *A. adsurgens* + *A. sacrorum* was

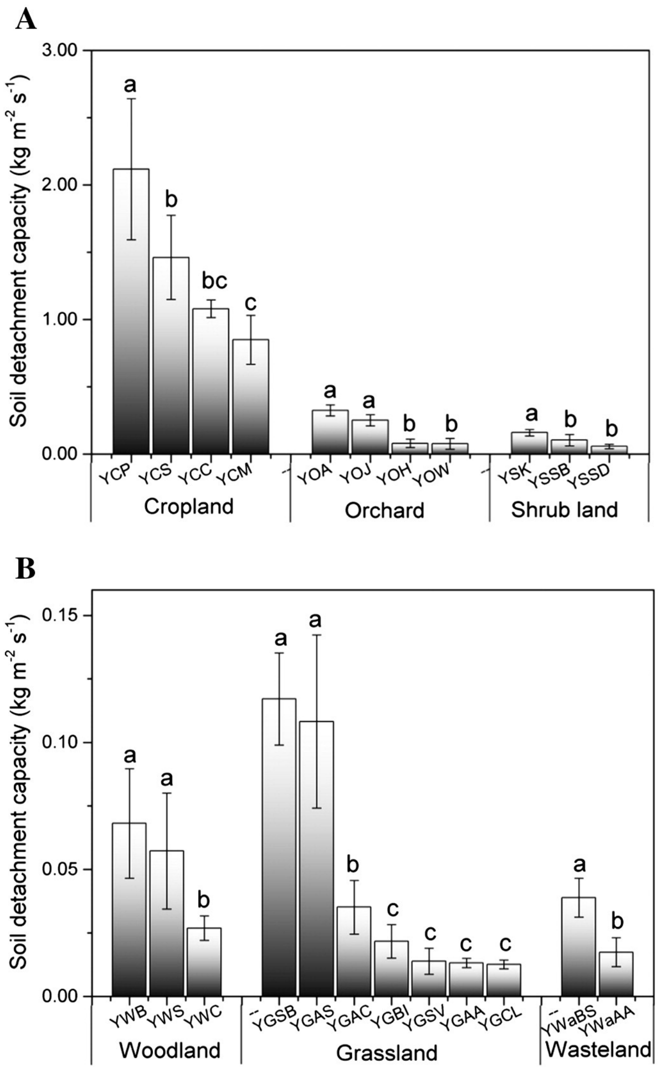

Fig. 4. Comparison of soil detachment capacities between different land uses on yellow loess soil. Error bars represent the standard deviation.

significantly less than that in *B. ischaemum* + *S. viridis* (Fig. 4B). This result was probably caused by soil biological crust development under *A. adsurgens* + *A. sacrorum*, although its organic matter and root density were less than those of *B. ischaemum* + *S. viridis* (Table 1).

3.3. Factors influencing soil detachment capacity

3.3.1. Hydraulic parameters

The statistical properties of the measured D_c under different shear stresses are shown in Table 3. It was found that the maximum soil detachment capacity of different land uses varied considerably from 0.117 to 4.427 kg m^{-2} s^{-1}; whereas the minimum D_c only ranged from 0 to 0.007 kg m^{-2} s^{-1}. Under each shear stress, the great standard deviations and coefficients of variation indicated a strong heterogeneity in soil detachment capacity between different sampling sites as strongly affected by soil types, land uses, and plant species. Soil detachment capacities measured under different shear stresses differed significantly (Table 3) and increased as a power function of either shear stress (Fig. 5A) or stream power (Fig. 5B) with a coefficient of determination of 0.42. This result is inconsistent with the conclusion of previous studies that stream power was better than shear stress to simulate soil detachment process (Nearing et al., 1999; Zhang et al., 2003).

3.3.2. Soil properties

Pearson correlation analysis showed that soil detachment capacity was positively correlated with silt content ($p < 0.01$), while it was negatively correlated with sand content ($p < 0.01$, Table 4). This result is in accordance with the findings of Knapen et al. (2007b) that soil with high silt content general showed a higher susceptibility for detachment. No statistical significant relationships were found between soil detachment capacity and clay content, median soil grain size, and bulk density ($p > 0.05$, Table 4). These results were probably resulted from the inclusion of the D_c variations caused by other factors such as land use in the statistical tests. Soil detachment capacity decreased with soil cohesion ($p < 0.01$, Table 4) as a power function (Fig. 6). This result is corroborated with the results of some recent studies (Wang et al., 2014a; Zhang et al., 2009b).

Both water stable aggregate and aggregate median diameter reflect the stability of soil, and have often been used as indicators of soil susceptibility to flowing water erosion (Barthes and Roose, 2002; Bissonnais, 1996). In this study, soil detachment capacity was influenced by water stable aggregate or aggregate median diameter significantly ($p < 0.01$, Table 4). The measured detachment capacity decreased as a power function of water stable aggregate with a coefficient of determination of 0.35 (Fig. 7). This result is different from the finding of Nearing et al. (1991). Soil detachment capacity was also closely related to soil organic matter ($p < 0.01$, Table 4) and a reverse relationship was detected between them. This result was in agreement with the conclusion of Knapen et al. (2007a).

3.3.3. Root systems

The correlation between soil detachment capacity and root mass density was significant ($p < 0.01$, Table 4), which implied that root density had a great impact on soil detachment capacity by overland flow. As shown in Fig. 8, it was obvious that soil detachment capacity decreased exponentially with an increase in root mass density. The coefficient of determination was 0.31. This erosion-reducing effect by root systems was also reported by De Baets et al. (2006) and Zhang et al. (2013). The decrease in detachment capacity mostly occurred in the root density range of 0 to 1 kg m^{-3}. When root density increased from 1 to 4 kg m^{-3}, the detachment capacity declined continuously but at a very low rate. When root density was greater than 4 kg m^{-3} the measured soil detachment capacity was almost stable. This result was somewhat different with the study of Zhang et al. (2013), in which most of D_c decline occurred when the root density was less than 4 kg m^{-3}. This difference

Table 3
Statistical parameters of measured soil detachment capacity under different shear stresses.

Shear stress (Pa)	Minimum (kg m^{-2} s^{-1})	Maximum (kg m^{-2} s^{-1})	Mean (kg m^{-2} s^{-1})	Standard deviation (kg m^{-2} s^{-1})	Coefficient of variation	*n*
5.51	0.000	0.117	0.013f	0.026	2.038	29
8.81	0.002	0.991	0.072e	0.185	2.554	29
10.26	0.002	1.672	0.166d	0.348	2.101	29
12.51	0.003	2.011	0.308c	0.528	1.716	29
14.88	0.007	3.533	0.453b	0.793	1.750	29
16.59	0.007	4.427	0.720a	1.242	1.726	29

Different letters indicate significant differences between shear stresses ($p < 0.05$).

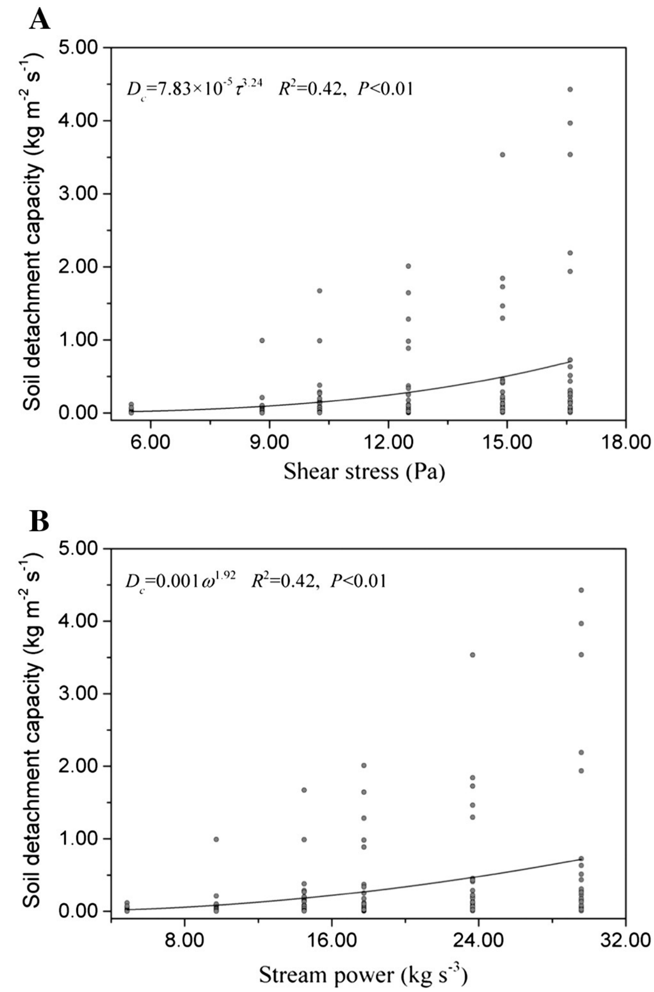

Fig. 5. Soil detachment capacity as a function of shear stress (A) and stream power (B).

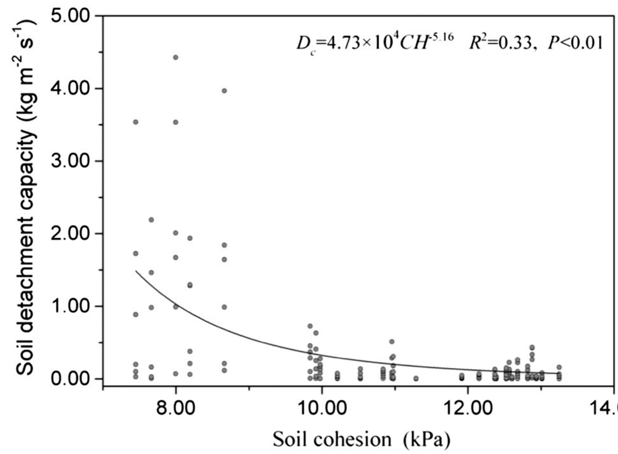

Fig. 6. Soil detachment capacity as a function of soil cohesion.

was probably caused by the differences in plant species, root diameter, and root architecture.

3.4. Soil detachment capacity estimation

Considering time-consuming and costly experiments of soil detachment capacity measurement in field conditions, it is imperative to develop a convenient and effective model based on some measureable hydraulic, soil, and vegetation parameters to estimate soil detachment capacity by overland flow in the Loess Plateau. Non-linear regression analysis showed that soil detachment capacity could be estimated by shear stress (τ, Pa), soil cohesion (CH, kPa), water stable aggregate (WSA, 0–1), and root density (RD, kg m^{-3}).

$$D_c = 0.06\tau^{2.83}CH^{-2.53}WSA^{-0.94}e^{-1.85RD} \quad R^2 = 0.84 \quad NSE = 0.84 \quad n = 174 \tag{5}$$

Generally, Eq. (5) predicted soil detachment capacity well with coefficient of determination (R^2) and Nash–Sutcliffe efficiency (NSE) of 0.84. For all dataset, the mean estimated detachment capacity was very close to the mean measured D_c and the ratio between them was 0.95. Nevertheless, considerable scatter was still found when soil detachment capacity was greater than 3 kg m^{-2} s^{-1} (Fig. 9A). When shear stress was replaced with stream power (ω, kg s^{-3}), a new equation was developed.

$$D_c = 0.57\omega^{1.69}CH^{-2.56}WSA^{-0.98}e^{-1.64RD} \quad R^2 = 0.84 \quad NSE = 0.83 \quad n = 174 \tag{6}$$

As expected, no any improvement was detected when stream power was used to estimate soil detachment capacity (Fig. 9B).

Torri et al. (1998) found that soil detachment by overland flow was closely related to stream power, and supposed the stable aggregate to be spherical, and then the following equation was developed to estimate soil detachment capacity:

$$D_c = \frac{\delta_s D_{50}\omega e}{1.5CHl} \tag{7}$$

where δ_s is the bulk density (kg m^{-3}), D_{50} is the aggregate median diameter (mm), and e/l is the function of clay content (%). Based on the finding of Torri et al. (1998), Ciampalini and Torri (1998) and Zhang et al. (2008) developed new equations to predict soil detachment capacity using hydraulic (stream power, slope gradient, and density of water) and soil parameters (bulk density, median diameter, clay content, and cohesion). However, the effect of root density on soil detachment capacity was neglected. For current study, nonlinear regression indicated (Fig. 10):

$$D_c = 0.35\frac{\delta_s D_{50}\omega}{\mathrm{CH}}\exp\left[0.02\frac{\mathrm{Silt}}{D_{50}} + 1.97S - 3.99\frac{\delta_s - \delta_w}{\delta_w} - 7.51\mathrm{RD}\right] \quad R^2 = 0.89 \quad \mathrm{NSE} = 0.89 \quad n = 174 \tag{8}$$

where $Silt$ is the silt content (%) and δ_w is the density of water (kg m^{-3}). Compared to Eqs. (5) and (6), the performance of Eq. (8) was improved and the R^2 and NSE were 0.89. Compared to Fig. 9, the notable scatter

Table 4
Pearson correlation coefficients between soil detachment capacity and soil properties, and root density.

Item	Clay (%)	Silt (%)	Sand (%)	Median soil grain size (μm)	Bulk density (kg m^{-3})	Soil cohesion (kPa)	Water stable aggregate (0–1)	Aggregate median diameter (mm)	Organic matter (g kg^{-1})	Root density (kg m^{-3})
D_c (kg m^{-2} s^{-1})	−0.015	0.437**	−0.240**	−0.037	−0.093	−0.547**	−0.463**	−0.402**	−0.351**	−0.316**

** Significant at $p < 0.01$ ($n = 174$).

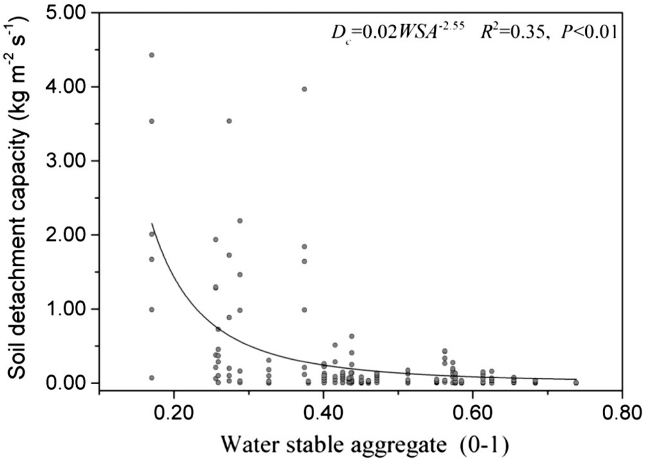

Fig. 7. Soil detachment capacity as a function of water stable aggregate.

disappeared when D_c was greater than 3 kg m^{-2} s^{-1}. Nevertheless, a slight worse in detachment capacity estimation was found when D_c was less than 1 kg m^{-2} s^{-1}.

4. Conclusions

Land use has great influence on soil detachment capacity by overland flow. However, its effects are not fully quantified in the Loess Plateau. This study was conducted to investigate the effects of land use on soil detachment capacity measured using undisturbed topsoil samples collected from 29 sites in a typical small watershed of the Loess Plateau. The result showed that D_c was strongly influenced by soil type. Yellow loess soil was more susceptible to detachment than red loess soil, and the mean D_c of yellow loess soil was 1.49 times greater than that of red loess soil. Similar to soil type, D_c was also affected by land use significantly. For red loess soil, D_c of cropland was the maximum and followed by shrub land, orchard, and grassland. For yellow loess soil, the mean soil detachment capacity of cropland was also the maximum, and was 7.14, 12.29, 25.78, 28.45, and 46.43 times greater than those of orchard, shrub land, woodland, grassland and wasteland, respectively. Soil detachment capacity was negatively related to sand content, soil cohesion, water stable aggregate, aggregate median diameter, soil organic matter, and root density, while it was positively related to shear stress, stream power, and silt content. Soil detachment capacity by overland flow could be well estimated ($NSE = 0.89$) by stream power, slope gradient, bulk density, D_{50}, silt content, cohesion, and root density. The results are helpful to understanding the mechanism

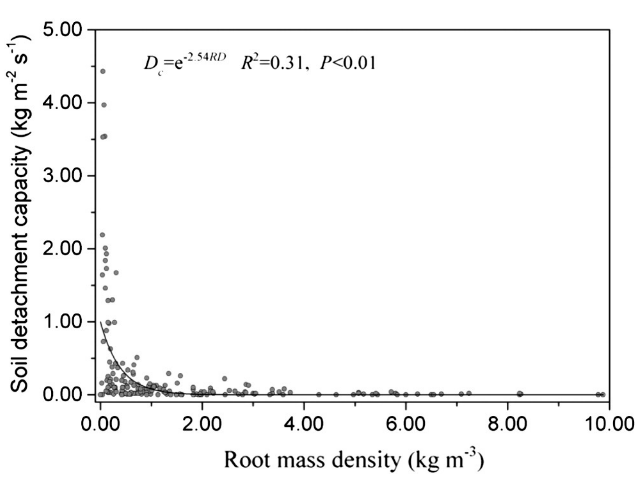

Fig. 8. Soil detachment capacity as a function of root density.

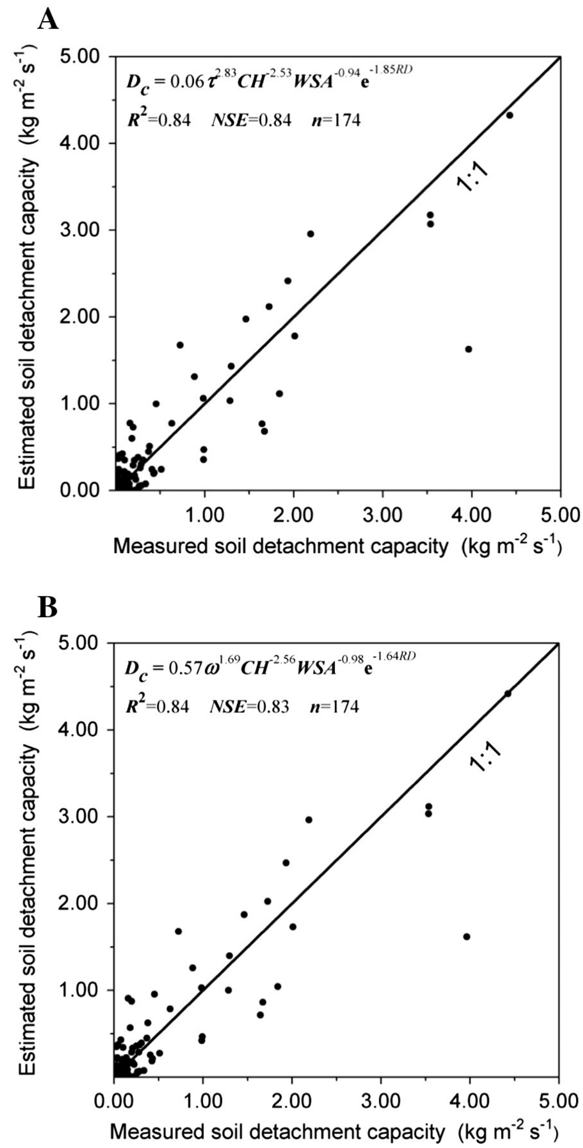

Fig. 9. Measured vs. estimated soil detachment capacities using Eqs. (5) (A) and (6) (B).

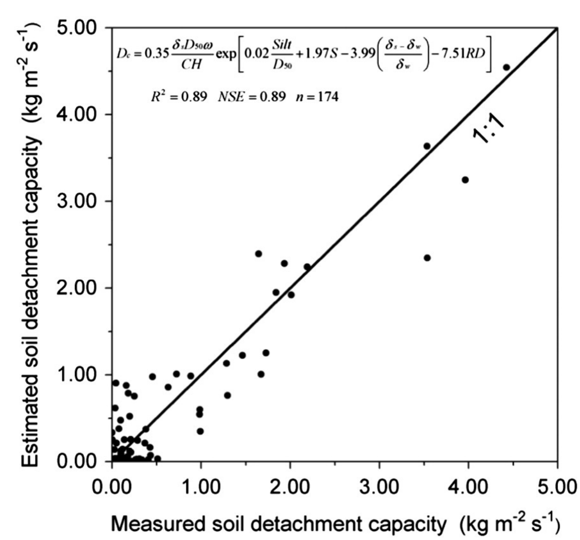

Fig. 10. Measured vs. estimated soil detachment capacities using Eq. (8).

of detachment process and to allocating soil conservation measures in small watershed of the Loess Plateau.

Acknowledgments

Financial assistance for this study was provided by the Hundred Talents Project of the Chinese Academy of Sciences and the National Natural Science Foundation of China (41271287 and 41301295). The authors thank the members of the Ansai Station of Soil and Water Conservation, Chinese Academy of Sciences and Ministry of Water Recourses for their assistance.

References

Barthes, B., Roose, E., 2002. Aggregate stability as an indicator of soil susceptibility to runoff and erosion; validation at several levels. Catena 47, 133–149.
Bissonnais, Y., 1996. Aggregate stability and assessment of soil crustability and erodibility: I. Theory and methodology. Eur. J. Soil Sci. 47 (4), 425–437.
Burylo, M., Rey, F., Mathys, N., Dutoit, T., 2012. Plant root traits affecting the resistance of soils to concentrated flow erosion. Earth Surf. Processes Landforms 37, 1463–1470.
Cao, L.X., Zhang, K.L., Zhang, W., 2009. Detachment of road surface soil by flowing water. Catena 76, 155–162.
Celik, I., 2005. Land-use effects on organic matter and physical properties of soil in a southern Mediterranean highland of Turkey. Soil Tillage Res. 83, 270–277.
Ciampalini, R., Torri, D., 1998. Detachment of soil particles by shallow flow: sampling methodology and observations. Catena 32, 37–53.
De Baets, S., Poesen, J., 2010. Empirical models for predicting the erosion-reducing effects of plant roots during concentrated flow erosion. Geomorphology 118, 425–432.
De Baets, S., Poesen, J., Gyssels, G., Knapen, A., 2006. Effects of grass roots on the erodibility of topsoils during concentrated flow. Geomorphology 76, 54–67.
De Baets, S., Poesen, J., Knapen, A., Galindo, P., 2007. Impact of root architecture on the erosion-reducing potential of roots during concentrated flow. Earth Surf. Processes Landforms 32, 1323–1345.
De Baets, S., Poesen, J., Meersmans, J., Serlet, L., 2011. Cover crops and their erosion-reducing effects during concentrated flow erosion. Catena 85, 237–244.
Franti, T., Laflen, J., Watson, D., 1999. Predicting soil detachment from high-discharge concentrated flow. Trans. ASAE 42, 329–335.
Fu, B.J., Chen, L.D., Ma, K.M., Zhou, H.F., Wang, J., 2000. The relationships between land use and soil conditions in the hilly area of the Loess Plateau in northern Shaanxi, China. Catena 39, 69–78.
Fu, B.J., Zhang, Q.J., Chen, L.D., Zhao, W.W., Gulinck, H., Liu, G.B., Yang, Q.K., Zhu, Y.G., 2006. Temporal change in land use and its relationship to slope degree and soil type in a small catchment on the Loess Plateau of China. Catena 65, 41–48.
García-Ruiz, J.M., 2010. The effects of land uses on soil erosion in Spain: a review. Catena 81, 1–11.
Ghebreiyessus, Y., Gantzer, C., Alberts, E., Lentz, R., 1994. Soil erosion by concentrated flow: shear stress and bulk density. Trans. ASAE 37, 1791–1797.
Govers, G., 1992. Relationship between discharge, velocity and flow area for rills eroding loose, non-layered materials. Earth Surf. Processes Landforms 17, 515–528.
Islam, K., Weil, R., 2000. Land use effects on soil quality in a tropical forest ecosystem of Bangladesh. Agric. Ecosyst. Environ. 79, 9–16.
King, K., Flanagan, D., Norton, L., Laflen, J., 1995. Rill erodibility parameters influenced by long-term management practices. Trans. ASAE 38, 159–164.
Knapen, A., Poesen, J., Govers, G., Gyssels, G., Nachtergaele, J., 2007a. Resistance of soils to concentrated flow erosion: a review. Earth Sci. Rev. 80, 75–109.
Knapen, A., Poesen, J., Galindo-Morales, P., De Baets, S., Pals, A., 2007b. Effects of microbiotic crusts under cropland in temperate environments on soil erodibility during concentrated flow. Earth Surf. Processes Landforms 32, 1884–1901.
Lei, T.W., Zhang, Q.W., Zhao, J., Xia, W.S., Pan, Y.H., 2002. Soil detachment rates for sediment loaded flow in rills. Trans. ASAE 45, 1897–1903.
Luk, S., Merz, W., 1992. Use of the salt tracing technique to determine the velocity of overland flow. Soil Technol. 5, 289–301.
Mamo, M., Bubenzer, G., 2001. Detachment rate, soil erodibility, and soil strength as influenced by living plant roots. Part I: laboratory study. Trans. ASAE 44, 1167–1174.
Nachtergaele, J., Poesen, J., 2002. Spatial and temporal variations in resistance of loess-derived soils to ephemeral gully erosion. Eur. J. Soil Sci. 53, 449–463.
Nearing, M., Foster, G., Lane, L., Finkner, S., 1989. A process-based soil erosion model for USDA-Water Erosion Prediction Project technology. Trans. ASAE 32, 1587–1593.
Nearing, M., Bradford, J., Parker, S., 1991. Soil detachment by shallow flow at low slopes. Soil Sci. Soc. Am. J. 55, 339–344.
Nearing, M., Simanton, J., Norton, L., Bulygin, S., Stone, J., 1999. Soil erosion by surface water flow on a stony, semiarid hillslope. Earth Surf. Processes Landforms 24, 677–686.
Pierret, A., Latchackak, K., Chathanvongsa, P., Sengtaheuanghoung, O., Valentin, C., 2007. Interactions between root growth, slope and soil detachment depending on land use: a case study in a small mountain catchment of Northern Laos. Plant Soil 301, 51–64.
Podwojewski, P., Orange, D., Jouquet, P., Valentin, C., Nguyen, V.T., Janeau, J.L., Tran, D.T., 2008. Land-use impacts on surface runoff and soil detachment within agricultural sloping lands in Northern Vietnam. Catena 74, 109–118.
Scherer, U., Zehe, E., Träbing, K., Gerlinger, K., 2012. Prediction of soil detachment in agricultural loess catchments: model development and parameterisation. Catena 90, 63–75.
Torri, D., Ciampalini, R., Gil, P.A., 1998. The role of aggregates on soil erosion processes. Presented at the "Global Changes: Modelling Soil Erosion by Water" Conference, NATO ARW. Oxford, U.K., October 1995.
Wang, J.G., Li, Z.X., Cai, C.F., Yang, W., Ma, R.M., Zhang, G.B., 2012. Predicting physical equations of soil detachment by simulated concentrated flow in Ultisols (subtropical China). Earth Surf. Processes Landforms 37, 633–641.
Wang, B., Zhang, G.H., Shi, Y.Y., Zhang, X.C., Ren, Z.P., Zhu, L.J., 2013. Effect of natural restoration time of abandoned farmland on soil detachment by overland flow in the Loess Plateau of China. Earth Surf. Processes Landforms 38, 1725–1734.
Wang, B., Zhang, G.H., Shi, Y.Y., Zhang, X.C., 2014a. Soil detachment by overland flow under different vegetation restoration models in the Loess Plateau of China. Catena 116, 51–59.
Wang, B., Zhang, G.H., Zhang, X.C., Li, Z.W., Su, Z.L., Shi, Y.Y., Yi, T., 2014b. Effects of near soil surface characteristics on soil detachment by overland flow in a natural succession grassland. Soil Sci. Soc. Am. J. 78, 589–597.
Zhang, G.H., Liu, B.Y., Liu, G.B., He, X.W., Nearing, M., 2003. Detachment of undisturbed soil by shallow flow. Soil Sci. Soc. Am. J. 67, 713–719.
Zhang, G.H., Liu, G.B., Tang, K.M., Zhang, X.C., 2008. Flow detachment of soils under different land uses in the Loess Plateau of China. Trans. ASABE 51, 883–890.
Zhang, G.H., Tang, K.M., Zhang, X.C., 2009a. Temporal variation in soil detachment under different land uses in the Loess Plateau of China. Earth Surf. Processes Landforms 34, 1302–1309.
Zhang, G.H., Liu, Y.M., Han, Y.F., Zhang, X.C., 2009b. Sediment transport and soil detachment on steep slopes: II. Sediment feedback relationship. Soil Sci. Soc. Am. J. 73, 1298–1304.
Zhang, G.H., Tang, K.M., Ren, Z.P., Zhang, X.C., 2013. Impact of grass root mass density on soil detachment capacity by concentrated flow on steep slopes. Trans. ASABE 56, 927–934.